Journal of Molecular Spectroscopy 388 (2022) 111686

Contents lists available at ScienceDirect

Journal of Molecular Spectroscopy

journal homepage: www.elsevier.com/locate/yjmsp

# Chirped-pulse Fourier-transform millimeter-wave rotational spectroscopy of furan in its $\nu_{10}$ and $\nu_{13}$ excited vibrational states

Piyush Mishra [*], Alexander W. Hull, Timothy J. Barnum [1], Brett A. McGuire, Robert W. Field

*Department of Chemistry, Massachusetts Institute of Technology, 77 Massachusetts Avenue, Cambridge MA-02139, USA*

A B S T R A C T

Furan, a prototypical heteroaromatic cyclic ether, is an important molecule that has garnered attention from a wide range of fields, from food and health research to combustion and atmospheric chemistry. Chirped-pulse Fourier-transform rotational spectroscopy of jet-cooled furan in the W-band across three narrow regions 79.3–79.45 GHz, 88.6–88.8 GHz, and 97.95–98.15 GHz is reported here. A pyrolysis nozzle was used to efficiently populate vibrationally excited states of low-frequency modes. Apart from the v = 0 state, vibrationally excited v = 1 states of modes $\nu_{11}$, $\nu_{14}$, $\nu_{10}$, and $\nu_{13}$ were observed. Furan is a planar molecule and these observed excited state modes correspond to out-of-plane vibrations. The v = 0 state and the vibrationally excited $\nu_{11}$ and $\nu_{14}$ were previously recorded and fit by Barnum et al (T. J. Barnum, K. L. K. Lee, B. A. McGuire, ACS Earth Space Chem. 5 (2021), 2986–2994). Rotational transitions in the J"=5 to 9 rotational states were fit for the previously undetected $\nu_{10}$ mode and experimental linelists for v = 1 states of modes $\nu_{10}$ and $\nu_{13}$ are provided, both of which are out-of-plane CH bending modes. Inertial defect was shown to be a useful quantity to extract structural information of vibrational modes of planar asymmetric tops. These rotational fits will assist astronomical searches for furan and its vibrational states.

## 1. Introduction

Furan (c-$C_4H_4O$) is a planar, heterocyclic, aromatic, 5-membered ring compound. Furan has attracted attention from many distinct fields. It is widely used as an organic solvent in synthetic chemistry and as a combustion control compound [1]. It is present as a volatile organic compound (VOC) in the atmosphere [2,3] and, at trace levels, as a flavorant in food[3,4]. Furan and its derivatives are air pollutants[5] that are classified as persistent organic pollutants,[6–8] and have been involved in environmental disasters[9]. Furan also has harmful health effects and is possibly carcinogenic in large quantities.[3,4] As the prototypical cyclic ether and the smallest stable heteroaromatic molecule, furan is attractive for fundamental research. Specifically in the gas phase, furan is a molecule of interest in astrochemistry, atmospheric chemistry, and combustion chemistry.

Five-membered unsaturated heterocycles, such as furan, are essential precursors to the formation of nucleic acids, which are essential building blocks of life.[10] In addition, furanose is a non-aromatic derivative of furan that is involved in nucleotide synthesis.[11] Although not yet detected in the interstellar medium (ISM), furan is an astrochemically relevant molecule, predicted to exist in a range of different environments.[12,13] Terrestrially, furan is thermally generated in processes such as cooking and combustion.[2–4,14,15] Given its relevance to multiple areas of research, furan reactivity and its production in gas-phase chemistry has garnered much attention. It has been a subject of fundamental research,[16–25] and research focused on atmospheric chemistry,[26–31] combustion chemistry,[32–34] and astrochemistry[35,36].

Furan, belonging to the $C_{2v}$ point group, is a near-oblate top with an a-axis dipole. As noted by Mellouki et al,[37] there has been confusion regarding assignments of the symmetry labels $B_1$ and $B_2$ in the $C_{2v}$ point group, and this confusion is evident across the spectroscopic literature involving furan.[35,37–41] The updated symmetry labels, defined by Bunker and Jensen,[42] which are in agreement with IUPAC recommendations,[43] were followed in more recent studies.[35,38] The updated list of normal modes and symmetry labels, along with figures that describe the vibrational modes, can be found in the article by Mellouki et al.[37] Previous work on furan using pure rotational and rotationally resolved spectroscopies has been performed on the ground vibrational state and several low-lying vibrational states. The ground state of furan, including its $^{13}C$ and deuterated isotopologues, have been well characterized via rotational spectroscopy.[35,44–47] The two lowest frequency vibrational modes $\nu_{11}$ ($A_2$) and $\nu_{14}$ ($B_1$) have also been studied, including a Coriolis interaction.[35,38] Higher frequency modes, $\nu_{13}$ ($B_1$),[39] $\nu_7$ ($A_1$),[48] $\nu_{18}$ ($B_2$),[38] $\nu_{19}$ ($B_2$),[38] and $\nu_6$ ($A_1$) [49], have been studied as well by infrared (IR) spectroscopy.

* Corresponding author.
*E-mail address:* mishrap@mit.edu (P. Mishra).
[1] Current address: Department of Chemistry, Union College, Schenectady, NY-12308, USA.

https://doi.org/10.1016/j.jms.2022.111686
Received 8 April 2022; Received in revised form 21 June 2022; Accepted 25 July 2022
Available online 28 July 2022

Still, the rotational structure of several lower frequency vibrational modes of furan remains unexplored. Some of these vibrational modes involve symmetry-forbidden transitions from the ground state. They are thus inaccessible to rotationally-resolved optical or high-resolution IR spectroscopic techniques. Pure-rotational spectroscopy, however, is not subject to such symmetry restrictions, as the rotational transitions occur within the same vibrational state. We performed pure-rotational spectroscopy on furan seeded in a pulsed helium supersonic jet, using a chirped-pulse Fourier-transform millimeter-wave (CP-FTmmW) spectrometer in an effort to further explore the ro-vibrational landscape of furan. With its multiplexed detection scheme, the rate of data acquisition for CP-FTmmW is about 1000 times faster than a frequency-tuned cavity spectrometer, the previous state-of-the-art technique.[50,51] A heated pyrolysis nozzle was used to observe rotational transitions in vibrationally excited states, called vibrational satellites.

We observed pure rotational transitions in the ground state as well as in four of the lowest-frequency vibrational modes. The fits of the ground state and the $\nu_{11}$ ($A_2$, 600 $cm^{-1}$) and $\nu_{14}$ ($B_1$, 603 $cm^{-1}$) out-of-plane ring deformation modes were taken from the CP-FTmmW work by Barnum et al.[35] The fit for the out-of-plane CH bending mode $\nu_{13}$ ($B_1$, 745 $cm^{-1}$) was obtained from high-resolution IR spectroscopy work by Pankoke et al.[39] Vibrational satellites of the previously unobserved $\nu_{10}$ ($A_2$, 721 $cm^{-1}$) mode, which is also an out-of-plane CH bending mode (Fig. 1), were detected within our spectra and the transitions were fit. This work also demonstrates the utility of the Chen-type pyrolysis nozzle[52] to populate and study vibrationally excited states in a supersonic jet, which are otherwise difficult to detect.[35].

We are also aware of a combined high-resolution IR and mm-wave study of the ground state and vibrationally excited states of furan that is currently underway, using data collected at the University of Wisconsin-Madison and the Canadian Light Source.[53] The millimeter wave (mmW) experiments are being carried out in a static cell, in the 130–375 GHz region. We view our work as complementary to this more extensive study, because many radio telescopes operate in the W-band region that we exploit in this study. Additionally, our work is performed at cold temperatures similar to the rotational temperature of the ISM (~5–10 K).[54,55] We hope that our rotational fit of $\nu_{10}$ and linelists of $\nu_{10}$ and $\nu_{13}$ vibrational satellites of furan, from experiments carried out under supersonic conditions, will be useful in the ongoing astrochemical searches.

## 2. Methods

In this study, we carried out spectroscopic measurements, compared the results with *ab initio* calculations, and fitted our spectrum to obtain experimental rotational parameters. The instrument is described in detail elsewhere,[35,57] and only the essential aspects are presented here. The instrument consists of three parts: (1) the vacuum chamber, (2) the pulsed valve outfitted with a pyrolysis nozzle, and (3) the CP-FTmmW spectrometer. Rotational spectra were recorded in the 75.6–99.6 GHz region.

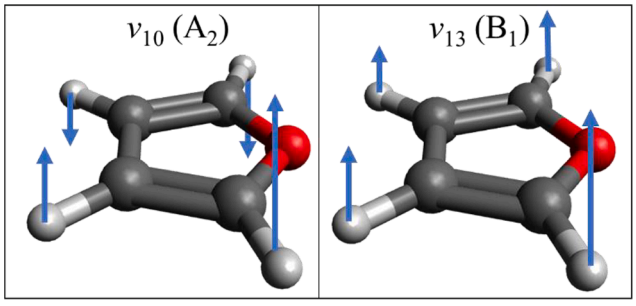


**Fig. 1.** Vibrational modes of furan fit in the present study [56]. The mode label along with their respective symmetries in brackets are at the top of the structures. The arrows represent the H atom displacements of the C—H out-of-plane bending modes.

### 2.1. Vacuum chamber and sample inlet

Commercially available furan (Sigma-Aldrich, ≥99 %) was used without further purification. As a liquid with high vapor pressure (~0.9 bar at 300 K), high concentrations of furan can be prepared in the gas phase.[58] Furan vapor (0.34 bar) was mixed (5 %) with helium (6.6 bar), creating a mixture that was used in our experiments at a backing pressure of 2 bar. A pulsed General Valve (Parker General Valve Series 9) with an 0.5 mm orifice diameter was used as the gas inlet. The vacuum chamber was evacuated using a 10-inch diffusion pump (Varian VHS-10). The base pressure of the chamber was ~ $1x10^{-6}$ Torr, and the operating pressure was ~ $5x10^{-4}$ Torr.

To observe vibrationally excited states, the orifice was outfitted with a Chen-type pyrolysis nozzle to heat the sample prior to expansion.[52,57] This heated extension to the pulsed valve, is made up of a 5.7 cm long SiC tube (Saint-Gobain) with 1 mm inner diameter. The SiC tube was resistively heated by a dc power supply (B&K Precision 1672), which can be tuned up to 1800 K. Temperature was optimized and maintained at ~ $400^{O}$C (~675 K), as measured by a W/Re type-C thermocouple (5 % measurement accuracy). The temperature-sensitive components of the General Valve were protected from the heated SiC tube by a water-cooled baffle. The output from the pyrolysis nozzle is directed perpendicular to the beam of frequency-chirped mmW radiation. The temperature of this heated SiC tube was optimized to maximize the signal intensities from the known $\nu_{11}$ and $\nu_{14}$ vibrational satellites.

### 2.2. CP-FTmmW spectrometer

The CP-FTmmW spectrometer consists of two arms: the up-conversion arm, responsible for broadcasting chirps in a suitable frequency region, and the down-conversion arm, responsible for detection of the molecular signal. To achieve phase-stability, a single phase-locked dielectric resonator oscillator (PLDRO, Miteq DLCRO-010–09375-3-15P), operating at 9.375 GHz, is used as the local oscillator (LO) on both arms. For the up-conversion arm, frequency chirps are generated by mixing the PLDRO output with the waveform from channel 1 of the arbitrary waveform generator (AWG, Agilent Technologies, M8190A). After up-conversion, the chirps are broadcast into the vacuum chamber using a rectangular W-band horn. The chirped mmW radiation intersects with the jet in a transverse geometry and polarizes the molecular rotational transitions. The molecular signal, in form of a free induction decay (FID), is collected. A rooftop reflector, placed inside the chamber rotates the polarization of the FID and reflects it back onto a wire-grid polarizer placed outside the chamber in front of the broadcast horn. This polarizer reflects the molecular FID signal onto the receiving horn. The 9.375 GHz radiation from the PLDRO mixes with a 2 GHz single frequency continuous wave output from the channel 2 of the AWG, generating the LO for the down-conversion arm. The amplified molecular FID (LNA, Millitech, LNA-10–02150) is mixed with this LO and the output is sent to an oscilloscope (Tektronix, DPO72004), resulting in a phase-coherent average in the time domain. All of the mmW electronics are referenced to a 10 MHz Rb clock (Stanford Research Systems FS725). For the details of the spectrometer, the reader can refer to Barnum et al.[35].

### 2.3. Spectral simulation and ab initio calculation

The PGOPHER spectral simulation program[59] was used to fit experimental observations against predicted transition frequencies. Because furan is a near-oblate symmetric top, Watson's S-reduced Hamiltonian was used in the $III^r$ representation ($S/III^r$).[59] Furan experimental molecular constants corresponding to rotational transitions in the ground, $\nu_{11}$, and $\nu_{14}$ vibrational states were obtained from Barnum et al.[35] For $\nu_{13}$, constants from Pankoke et al. were used.[39]

For previously unobserved low-frequency vibrational satellites, $\nu_{10}$, $\nu_{12}$, $\nu_9$, and $\nu_{21}$, rotational constants were obtained from *ab initio* calculations. *Ab initio* calculations on furan were performed using the CFOUR suite of programs.[60] Geometry optimization and anharmonic frequency calculations were performed to obtain the rotational constants that correspond to the observed vibrational satellites. Coupled-cluster theory with perturbative triple excitations [CCSD(T)] under the frozen-core (fc) approximation was employed, using the ANO0 basis set.[61] Due to the presence of identical nuclei, the nuclear spin statistics effect was observed in the relative intensities in the spectral simulation, as described by Barnum et al.[35] Rotational and vibrational temperatures were approximated from the observed relative intensities in the experimental spectrum.[59].

### 2.4. Chirps and data post-processing

The frequency chirps were 1 μs in length and were scanned over the three narrow ranges of 79.3–79.45 GHz, 88.6–88.8 GHz, and 97.95–98.15 GHz, in three separate experiments, as the most intense furan rotational transitions were determined to occur in those regions. The bulk of the molecular signal resided within the first 2 μs of the FID, detection of which started after a delay of 0.5 μs after the end of the excitation chirp, in order to minimize detection of ringing from the LNA. The spectral resolution is 0.5 MHz. The full-width at half maximum (FWHM) of the observed lines was 1 MHz, which was input as the transition width in the PGOPHER spectral simulation. 2 million averages were collected over each of the three frequency regions. A fast Fourier transform of the averaged FID was performed in MATLAB (R 2020a).[62] A Gaussian windowing function was used (window parameter 2.5). Instrument artifacts were removed from the final experimental spectrum.

## 3. Results and discussion

Rotational spectra of the furan ground state and the v = 1 excited vibrational states in modes $\nu_{11}$, $\nu_{14}$, $\nu_{10}$, and $\nu_{13}$, were obtained within our spectral region (79.3–79.45 GHz, 88.6–88.8 GHz, and 97.95–98.15 GHz). Portions of the spectra are shown in Fig. 2. These spectra were recorded with the pyrolysis nozzle maintained at ~ 400$^{O}$C (~675 K). At ~ 600$^{O}$C (~875 K), no furan transitions were observed, presumably due to thermal decomposition.[34] The PGOPHER simulated spectra (pointed downwards), with Gaussian peak width set at 1 MHz, match well with the experimental spectra (pointed upwards). Our spectra is Doppler broadened due to the perpendicular intersection between the jet and the beam of mmW chirped radiation.[63] Experimental constants from Barnum et al. were used for modes $\nu_{11}$ and $\nu_{14}$, the line-centers of which matched well with our observed transitions (Fig. 2).[35] The rotational transition fitting was performed for modes $\nu_{10}$ and $\nu_{13}$ over the range of J"=5 to 9 (Table 1).

Pankoke et al. have fit a large number of $\nu_{13}$ lines (3500), which includes quartic and sextic distortion coefficients, using Watson's A-reduced Hamiltonian in the I$^{r}$ representation (A/I$^{r}$).[39] By contrast, we fit our experimental data for $\nu_{10}$ and $\nu_{13}$ in (S/III$^{r}$). Henceforth we will use the shorthand (Watson's reduced Hamiltonian letter/Axis representation) for ease. We chose this combination of reduction and representation for consistency with and for easy comparison to the fits of the ground state, and the v = 1 vibrational levels of modes $\nu_{11}$, and $\nu_{14}$ reported by Barnum et al., where the experiments were carried out in the same spectrometer as used in this study.[35] Pankoke et al. observed only c-type transitions, and we observe exclusively a-type transitions, which makes our pure rotation spectrum complementary to high-resolution IR spectrum.[39] We report the linelist from our pure-rotational spectroscopy in the **Supplementary Information**, obtained at higher resolution (0.5 MHz) than the high-resolution IR work by Pankoke et al. (60 MHz).[39].

Detailed investigation carried out by Demaison and co-workers show that III$^{r}$ representation together with Watson's A-reduced Hamiltonian (A/III$^{r}$) is often a poor choice.[64,65] Neither Pankoke et al., nor the present work used this combination for fitting the vibrationally excited states of furan.[39] Moreover, fitting of the ground state of furan by Margulès et al using (S/III$^{r}$), showed the best results with the least standard deviation, which is the same fitting condition used in the present study.[65] Our observations for the $\nu_{13}$ state of furan, were fit at (S/III$^{r}$) and (A/I$^{r}$), both of which converged to the same values for the set of small molecular parameters (Table 1).

We observed 12 resolved transitions for the $\nu_{10}$ and 10 resolved transitions for the $\nu_{13}$ modes in their v = 1 states, in addition to a nearly blended transition in the $\nu_{10}$ state. Apart from these 22 transitions, we observed vibrational satellites from the v = 1 levels of modes $\nu_{10}$ and $\nu_{13}$ that were fully blended with transitions from other vibrational satellites (Fig. 2). Transitions with signal-to-noise < 3 were de-weighted by a factor of 2. For near-symmetric tops, as the difference between the J and K quantum numbers increases, the splittings in the K-stack increases. The vibrational satellite transitions for furan (near-oblate asymmetric top) where J - K$_c$ = 0 or 1, were unresolved in our spectrum, and hence were among the most intense peaks. Such J-K$_c$ ≤ 1 transitions were, therefore, very useful in the initial stages of the fitting process, after which the other a-type resolved lines were fit. Such blended lines with multiple transition assignments were fit to the mean position.[59] The *ab initio* calculations predicted the rotational constants of the v = 1 levels of modes $\nu_{10}$ and $\nu_{13}$ to a high accuracy (Table 1, within 0.45 MHz). Our experimental spectrum, final fits, and linelist are available in **Supplementary Information**. Efforts to identify transitions in the next higher energy vibrational states, the in-plane ring modes, $\nu_8$ (A$_1$, 871 cm$^{-1}$) and $\nu_{21}$ (B$_2$, 873 cm$^{-1}$), were unsuccessful.

As mentioned previously, we also used (A/I$^{r}$) to fit the $\nu_{13}$ state of furan, which converged to the same molecular constants as the fit performed using (S/III$^{r}$) (Table 1). This is because the quartic terms in both Watson's A-reduced and S-reduced Hamiltonians have the same expression.[64,65] Pankoke et al. fit 12 molecular parameters, whereas we fit 4.[39] Meaningful comparison cannot be performed between fits generated using very different number of parameters, as the fits get projected into parameter space with different dimensions. In other words, the interdependence of these parameters makes the comparison less meaningful. Nevertheless, the ground and vibrationally excited states of asymmetric tops can be compared using their inertial defects (Δ), calculated from the respective moments of inertia (**Equation (1)**).

$$\Delta = I_C - I_B - I_A \quad (1)$$

The inertial defect is a particularly useful quantity to compare the geometries of various states of an asymmetric top molecule, because they are largely independent of centrifugal and electronic distortion contributions.[66] For planar asymmetric tops, the inertial defect of the vibrational ground state geometry is very close to 0, while the inertial defects for the in-plane vibrations are typically large and positive and those for the out-of-plane vibrations are typically small and negative. Very low frequency, out-of-plane vibrational modes that exist in non-rigid molecules, like torsional modes are an exception to this trend.[66].

Being a planar molecule, we see that the inertial defect of the ground state of furan is 0.0488, which is very close to 0. Furthermore, being a rigid molecule, the 4 lowest energy vibrational modes ($\nu_{11}$, $\nu_{14}$, $\nu_{10}$, and $\nu_{13}$) corresponding to out-of-plane motions, have small negative inertial defects (Table 2). The largest departure from planarity is observed for $\nu_{14}$ (B$_1$), followed closely by $\nu_{11}$ (A$_2$), both of which are out-of-plane ring deformation modes. The slightly larger inertial defect of these modes agrees with the displacement of the heavier C-atoms in the skeletal framework. In contrast for $\nu_{10}$ and $\nu_{13}$ modes, primarily the light H-atoms are displaced, causing a smaller inertial defect among the 4 lowest vibrationally excited states of furan (Fig. 1).

At the nozzle temperature (T$_{noz}$) of 675 K, the rotational temperature is found to be ~ 15 K, which is higher than that reported by Barnum et al. (~5 K), because a pyrolysis nozzle was used in this work to observe

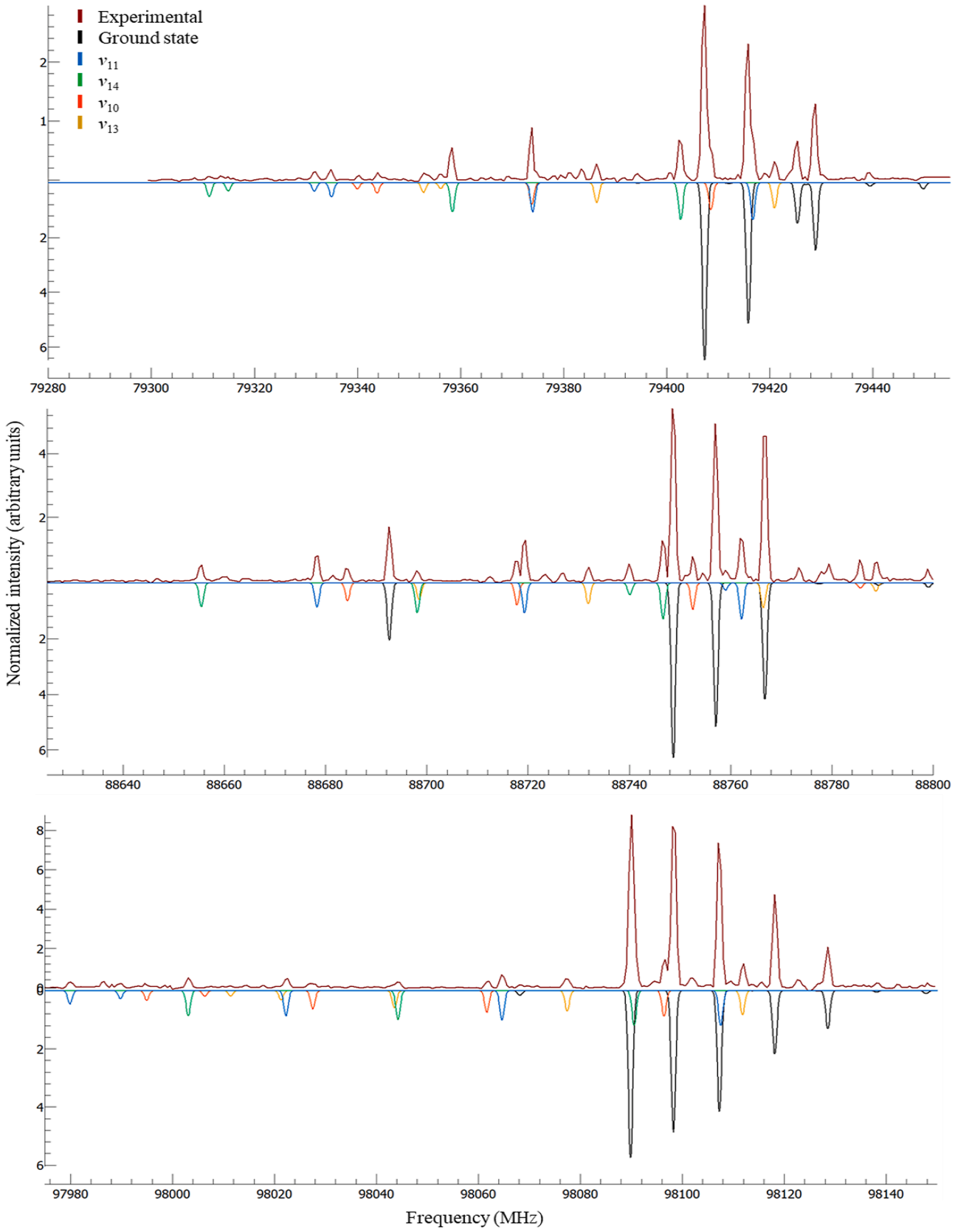


**Fig. 2.** Rotational spectra of furan in three 175 MHz wide regions: 79280–79455 MHz (top), 88625–88800 MHz (middle), and 97975–98150 MHz (bottom). Experimental spectra (maroon) are directed up and PGOPHER [59] simulated spectra are directed down. The simulations show the rotational transitions in the vibrational ground state (black), $v_{11}$ (blue), $v_{14}$ (green), $v_{10}$ (orange), and $v_{13}$ (yellow). The transition FWHMs are 1 MHz.

**Table 1**
Rotational fit parameters for $\nu_{10}$ and $\nu_{13}$ v = 1 vibrational states of furan in MHz. Our experimental fits were performed in III$^r$ representation using Watson's S-reduced Hamiltonian. Pankoke et al. [39] used I$^r$ representation and Watson's A-reduced Hamiltonian for the $\nu_{13}$ fit, which are italicized. Standard deviations of the last two significant digits are shown in parentheses. Number of lines fit ($N_{fit}$) and the number of unique frequencies ($N_{freq}$) are shown.

| Molecular constants | $\nu_{10}$ ($A_2$, 721 cm$^{-1}$) | | $\nu_{13}$ ($B_1$, 745 cm$^{-1}$) | | |
|---|---|---|---|---|---|
| | *ab initio* | This work | *ab initio* | Ref. [39] | This work |
| A | 9430.989 | 9430.578 (58) | 9427.127 | *9427.7517 (38)* | 9427.477 (50) |
| B | 9225.336 | 9225.090 (91) | 9231.556 | *9231.2821 (30)* | 9231.175 (82) |
| C | 4671.849 | 4672.194 (36) | 4672.475 | *4672.9007 (22)* | 4672.892 (13) |
| $D_J$ / $\Delta_J$ (x10$^3$) | | 0.48(17) | | *1.7276(32)* | 0.343(72) |
| $D_{JK}$ / $\Delta_{JK}$ (x10$^3$) | | | | *−0.215 (11)* | |
| $D_K$ / $\Delta_K$ (x10$^3$) | | | | *1.784(12)* | |
| $\delta_J$ (x10$^3$) | | | | *0.68603 (74)* | |
| $\delta_K$ (x10$^3$) | | | | *1.2478(24)* | |
| $\Phi_J$ (x10$^6$) | | | | *0.0016(14)* | |
| $\Phi_{JK}$ (x10$^6$) | | | | *−0.0102 (71)* | |
| $\Phi_{KJ}$ (x10$^6$) | | | | *0.023(14)* | |
| $\Phi_K$ (x10$^6$) | | | | *−0.0183 (96)* | |
| $N_{fit}/N_{freq}$ | | 15/12 | | *3500* | 13/10 |
| rms (MHz) | | 0.177 | | | 0.108 |
| Reduced rmsd[a] | | 0.162 | | | 0.067 |

[a] [Σ((observed frequency-calculated frequency)/weight)$^2$]/($N_{fit}$)]$^{1/2}$ (unitless).

**Table 2**
Inertial defect (Δ) of ground and excited vibrational states of furan performed at Watson's S-reduced Hamiltonian with III$^r$ representation. The units of Δ is (amu × Angstrom$^2$) The inertial defect for the ground state, $\nu_{11}$ and $\nu_{14}$ v = 1 states were calculated from rotational constants obtained by Barnum et al.[35].

| Molecular state | Δ (amu Å$^2$) |
|---|---|
| Ground state ($A_1$) | 0.0488 |
| $\nu_{11}$ ($A_2$, 600 cm$^{-1}$) | −0.2486 |
| $\nu_{14}$ ($B_1$, 603 cm$^{-1}$) | −0.2687 |
| $\nu_{10}$ ($A_2$, 721 cm$^{-1}$) | −0.2051 |
| $\nu_{13}$ (B1, 745 cm$^{-1}$) | −0.2028 |

vibrational satellites.[35] The *vibrational* temperature ($T_{vib}$) of furan is ~ 500–600 K in the supersonic jet, having a non-thermalized distribution, as noticed by Barnum et al.[35] There are a few reasons for this: (1) vibrational energy transfer is mode-specific and vibrational relaxation (VR) under collisionally cooled conditions depends on the frequency of the given mode;[57,67] (2) the pyrolysis nozzle creates a far from homogeneous initial pre-expansion temperature, because there is no proper mixing of the gas flow near the wall of the tube with the gas flow near the centerline.[57,68].

Next we compare the VR of furan in our experiments with that of Barnum et al.[35] where a pyrolysis nozzle was not used. With $T_{noz}$ = 300 K, Barnum et al. observed $\nu_{11}$ and $\nu_{14}$ at a $T_{vib}$ = 250 K.[35] The extent of VR, quantified as the ratio $T_{vib}/T_{noz}$,[57] is about 0.8 in the present work as well as in Barnum et al.[35] This implies that a pyrolysis nozzle does not significantly affect the VR of the supersonic expansion at moderate temperatures of up to 700 K. The combination of a supersonic jet with a pyrolysis nozzle is uniquely suited to populate vibrationally excited states, while rotationally cooling the sample to ~ 10 K, populating the low J states, thereby enhancing the signal of the sample. Hence, this technique can be successfully used to efficiently populate and study vibrationally excited states under well characterized supersonic expansion conditions.[69] However at much higher $T_{noz}$ ~ 1500 K, enhanced VR is observed by Prozument et al.[57].

Furan has not yet been discovered in the ISM or in star-forming regions, but its existence is anticipated, as cyclic oxygen containing compounds like ethylene oxide (c-$C_2H_4O$)[70,71] and propylene oxide ($CH_3C_2H_3O$),[72] and aromatic compounds[55,73–75] have been detected in the ISM. There have been several searches for furan and upper limit estimations of its concentration.[13,76] Even though the ISM is a low temperature region (~5–10 K),[54,55] furan can exist in hot star-forming regions where temperatures are a few 100s of K,[12,77] and in highly non-thermal environments,[78] where vibrationally excited states are expected to be populated. Upon detection of furan in outer space, the fits and experimental linelist of its vibrational satellites, provided by our work, will be very important to understand the various environments of its occurrence and to estimate its concentration accurately.

Adding the large linelist (about 3500 transitions) corresponding to the $\nu_{13}$ mode (v = 1) of furan, that was recorded by Pankoke et al., was not feasible, as the linelist was not available in the publication.[39] Therefore we adopted a method to assimilate and rationalize fits obtained in dissimilar experiments at very different resolutions (0.5 MHz in the present pure-rotational spectroscopy study and 60 MHz in the high-resolution IR study by Pankoke et al.), toward a global fit of the $\nu_{13}$ state.[39] The linelist of $\nu_{13}$ from the present work in the W-band region is used. The fit provided by Pankoke et al. has been used to simulate a spectrum of the $\nu_{13}$ = 1 state of furan.[39] This simulated linelist hence obtained, is taken to be the 'observed' linelist in the global fit, with the appropriate weights. With a larger number of lines available, a greater number of molecular parameters were fit (Table 3). The results in Table 3 show the similarity between the rotational constants of the global fit and the fit by Pankoke et al. in Table 1.[39] The low reduced root-mean-square deviation value is due to the large number of lines used, despite a large rms. To the knowledge of the authors, this is a previously untried method to integrate fits, the results of which appear to reasonably agree with the fit by Pankoke et al. (Table 1).[39] The specific details are provided in **Supplementary Information**.

## 4. Conclusion

We recorded broadband rotational spectra of furan in the millimeter wave region (75.6–99.6 GHz). Our search was focused on three narrow regions (79.3–79.45 GHz, 88.6–88.8 GHz, and 97.95–98.15 GHz),

**Table 3**
Rotational global fit parameters for $\nu_{13}$ v = 1 vibrational state of furan in MHz. Experimental fits were performed in Watson's S-reduced Hamiltonian using III$^r$ representation. This global fit was obtained by assimilating our $\nu_{13}$ fit with the fit by Pankoke et al[39]. Standard deviations of the last two significant digits are shown in parentheses. Number of lines fit ($N_{fit}$) and the number of unique frequencies ($N_{freq}$) are shown.

| Molecular constants | $\nu_{13}$ ($B_1$, 745 cm$^{-1}$) |
|---|---|
| A | 9427.7160(21) |
| B | 9231.2896(26) |
| C | 4672.89850(52) |
| $D_J$ (x10$^3$) | 3.2535(25) |
| $D_{JK}$ (x10$^3$) | −5.1003(28) |
| $D_K$ (x10$^3$) | 2.1958(30) |
| Δ (amu Å$^2$) | −0.2009 |
| $N_{fit}/N_{freq}$ | 1323/901 |
| rms (MHz) | 0.504 |
| Reduced rmsd[a] | 0.0203 |

[a] [Σ((observed frequency-calculated frequency)/weight)$^2$]/($N_{fit}$)]$^{1/2}$ (unitless).

spanning transitions in rotational levels J"=5 to 9. In addition to the ground vibrational state, we observed previously reported rotational fits in the v = 1 levels of the $\nu_{11}$, $\nu_{14}$, and $\nu_{13}$ vibrational modes. We also observed and fit rotational transitions in the $\nu_{10}$ vibrational mode that had not been reported in the literature. We fit 4 rotational parameters (A, B, C, $D_J$) for $\nu_{10}$ and $\nu_{13}$ states using Watson's S-reduced Hamiltonian in the $III^r$ representation. Using inertial defects of furan at its ground and vibrationally excited states, we could meaningfully compare the type and extent of the deformation caused by the vibrational modes. This was shown to be a particularly useful quantity, when a limited number of fit parameters (rotational constants) are available. With 4 rotational constants fit to these v = 1 vibrational satellites, our experimental fits and data can be used by researchers in the gas-phase spectroscopy community as starting points toward more inclusive rotational fits. Apart from assisting astrochemical searches and potentially helping to monitor combustion and atmospheric chemistry, this study shows that a pulsed supersonic nozzle outfitted with a pyrolysis tube is a useful source of efficient vibrational excitation, that can be used to study rotationally cold vibrational states of isolated molecules. We have also attempted to integrate the fit for the $\nu_{13}$ state of furan obtained in this study with the work by Pankoke et al., despite non-inclusion of their experimental linelist.[39]

## Declaration of Competing Interest

The authors declare that they have no known competing financial interests or personal relationships that could have appeared to influence the work reported in this paper.

## Data availability

I have attached all the data and supporting program files in the supplementary information.

## Acknowledgement

P.M. was supported by US Department of Energy grant (SC0021580). A.W.H. was supported by National Science Foundation grant (CHE-1800410). T.J.B was supported by a Beckman Young Investigator Award made to B.A.M. by the Arnold and Mabel Beckman Foundation. We want to thank the UW-Madison group, in particular, Brian J. Esselman, R. Claude Woods, and Robert J. McMahon for providing us with their latest fits, which enabled us to confirm our assignments. We want to thank Kin Long Kelvin Lee for providing us with the ab initio calculations of excited vibrational states of furan.

## Appendix A. Supplementary data

Supplementary data to this article can be found online at https://doi.org/10.1016/j.jms.2022.111686.

## References

[1] N. Xu, J. Gong, Z. Huang, Review on the production methods and fundamental combustion characteristics of furan derivatives, Renew. Sust. Energ. Rev. 54 (2016) 1189–1211.
[2] M.J. Newland, Y. Ren, M.R. McGillen, L. Michelat, V. Daële, A. Mellouki, $NO_3$ chemistry of wildfire emissions: a kinetic study of the gas-phase reactions of furans with the $NO_3$ radical, Atmos. Chem. Phys. 22 (2022) 1761–1772.
[3] J. Vranová, Z. Ciesarová, Furan in Food - a review, Czech J. Food Sci. 27 (No. 1) (2009) 1–10.
[4] S. Santonicola, R. Mercogliano, Occurrence and production of furan in commercial foods, Ital. J. Food Sci. 28 (2016) 155–177.
[5] D. Vallero, Chapter 6-Inherent properties of air pollutants, Fundamentals of air pollution, 5th ed., Academic Press, 2014, pp. 139–195.
[6] S. Kanan, F. Samara, Dioxins and Furans: A review from chemical and environmental perspectives, Trends Environ, Anal. Chem. 17 (2018) 1–13.
[7] W.J. Shields, S. Ahn, J. Pietari, K. Robrock, L. Royer, Chapter 6-Atmospheric fate and behavior of POPs, Elsevier, Environmental forensics for persistent organic pollutants, 2014, pp. 199–289.
[8] E.J. Reiner, K.J. Jobst, D. Megson, F.L. Dorman, J.F. Focant, Chapter 3-Analytical methodology of POPs, Elsevier, Environmental forensics for persistent organic pollutants, 2014, pp. 59–139.
[9] M. Doble, A. Kumar, Chapter 2-Environmental Disasters, Elsevier, Biotreatment of industrial effluents, 2005, pp. 11–18.
[10] J. McMurry, Organic Chemistry, Boston (2016).
[11] N. Kitadai, S. Maruyama, Origins of Building Blocks of Life: A Review, Geosci. Front. 9 (4) (2018) 1117–1153.
[12] A. Occhiogrosso, A. Vasyunin, E. Herbst, S. Viti, M.D. Ward, S.D. Price, W. A. Brown, Ethylene oxide and acetaldehyde in hot cores, Astron. Astrophys. 564 (A123) (2014) 1–9.
[13] J.E. Dickens, W.M. Irvine, A. Nummelin, H. Møllendal, S. Saito, S. Thorwirth, Å. Hjalmarson, M. Ohishi, Searches for new interstellar molecules, including a tentative detection of aziridine and a possible detection of propenal, Spectrochim. Acta A Mol. Biomol. Spectrosc. 57 (4) (2001) 643–660.
[14] J. S. Lighty, J. M. Veranth, The role of research in practical incineration systems - A look at the past and the future, 27th Symposium (International) on Combustion/ The Combustion Institute (1998), 1255-1273.
[15] R. Barro, J. Regueiro, M. Llompart, C. Garcia-Jares, Analysis of industrial contaminants in indoor air: Part 1. Volatile organic compounds, carbonyl compounds, polycyclic aromatic hydrocarbons and polychlorinated biphenyls, J. Chromatogr. A. 1216 (3) (2009) 540–566.
[16] S. Al-Hammadi, G. da Silva, Thermal decomposition and isomerization of furfural and 2-pyrone: a theoretical kinetic study, Phys. Chem. Chem. Phys. 23 (3) (2021) 2046–2054.
[17] B. Cabañas, A. Tapia, F. Villanueva, S. Salgado, E. Monedero, P. Martín, Kinetic study of 2-Furanaldehyde, 3-Furanaldehyde, and 5-Methyl-2- furanaldehyde reactions initiated by Cl atoms, Int. J. Chem. Kinet. 40 (10) (2008) 670–678.
[18] A. Bierbach, I. Barnes, K.H. Becker, Rate coefficients for the gas-phase reactions of hydroxyl radicals with furan, 2-Methylfuran, 2-Ethylfuran and 2,5-Dimethylfuran at 300 ± 2 K, Atmos. Environ. 26 (5) (1992) 813–817.
[19] T.J. Wasowicz, M. Łabuda, B. Pranszke, Charge Transfer, Complexes Formation and Furan Fragmentation Induced by Collisions with Low-Energy Helium Cations, Int. J. Mol. Sci. 20 (6022) (2019) 1–20.
[20] K.M. Vogelhuber, S.W. Wren, L. Sheps, W.C. Lineberger, The C-H bond dissociation energy of furan: photoelectron spectroscopy of the furanide anion, J. Chem. Phys. 134 (064302) (2011) 1–8.
[21] A.E.P.M. Sorrilha, L.S. Santos, F.C. Gozzo, R. Sparrapan, R. Augusti, M.N. Eberlin, Intrinsic Reactivity of Gaseous Halocarbocations toward Model Aromatic Compounds, J. Phys. Chem. A 108 (34) (2004) 7009–7020.
[22] O. Sorkhabi, F. Qi, A.H. Rizvi, A.G. Suits, Ultraviolet photodissociation of furan probed by tunable synchrotron radiation, J. Chem. Phys. 111 (1) (1999) 100–107.
[23] T. Suzuki, Time-Resolved photoelectron spectroscopy of non-adiabatic electronic dynamics in gas and liquid phases, Int. Rev. Phys. Chem. 31 (2) (2012) 265–318.
[24] E. Erdmann, M. Łabuda, N.F. Aguirre, S. Díaz-Tendero, M. Alcamí, Furan fragmentation in the gas phase: new insights from statistical and molecular dynamics calculations, J. Phys. Chem. A 122 (16) (2018) 4153–4166.
[25] L.D. Fondren, N.G. Adams, L. Stavish, Gas phase reactions of $CH_3^+$ with a series of homo- and heterocyclic molecules, J. Phys. Chem. A. 113 (3) (2009) 592–598.
[26] B. Cabañas, M.T. Baeza, S. Salgado, P. Martín, R. Taccone, E. Martínez, Oxidation of heterocycles in the atmosphere: kinetic study of their reactions with $NO_3$ radical, J. Phys. Chem. A 108 (2004) 10818–10823.
[27] T. Berndt, O. Böge, W. Rolle, Products of the gas-phase reactions of $NO_3$ radicals with furan and tetramethylfuran, Environ. Sci. Technol. 31 (4) (1997) 1157–1162.
[28] T. Berndt, O. Böge, Atmospheric reaction of OH radicals with 1,3-butadiene and 4-hydroxy-2-butenal, J. Phys. Chem. A 111 (48) (2007) 12099–12105.
[29] J. Jiang, W.P.L. Carter, D.R. Cocker, K.C. Barsanti, Development and evaluation of a detailed mechanism for gas-phase atmospheric reactions of furans, ACS Earth and Space Chem. 4 (8) (2020) 1254–1268.
[30] S.M. Aschmann, N. Nishino, J. Arey, R. Atkinson, Products of the OH radical-initiated reactions of furan, 2- and 3-Methylfuran, and 2,3- and 2,5-Dimethylfuran in the presence of NO, J. Phys. Chem. A 118 (2) (2014) 457–466.
[31] C. Andersen, O.J. Nielsen, F.F. Østerstrøm, S. Ausmeel, E.J.K. Nilsson, M.P. Sulbaek Andersen, Atmospheric chemistry of Tetrahydrofuran, 2-Methyltetrahydrofuran, and 2,5-Dimethyltetrahydrofuran: Kinetics of Reactions with Chlorine Atoms, OD Radicals, and Ozone, J. Phys. Chem. A 120 (37) (2016) 7320–7326.
[32] D. Liu, C. Togbé, L.-S. Tran, D. Felsmann, P. Oßwald, P. Nau, J. Koppmann, A. Lackner, P.-A. Glaude, B. Sirjean, R. Fournet, F. Battin-Leclerc, K. Kohse-Höinghaus, Combustion Chemistry and flame structure of furan group biofuels using molecular-beam mass spectrometry and gas chromatography - Part I: Furan, Combust. Flame 161 (3) (2014) 748–765.
[33] T. Joo, J.C. Rivera-Rios, M. Takeuchi, M.J. Alvarado, N.L. Ng, Secondary organic aerosol formation from reaction of 3-Methylfuran with nitrate radicals, ACS Earth Space Chem. 3 (6) (2019) 922–934.
[34] K.N. Urness, Q. Guan, A. Golan, J.W. Daily, M.R. Nimlos, J.F. Stanton, M. Ahmed, G.B. Ellison, Pyrolysis of furan in a microreactor, J. Chem. Phys. 139 (2013), 124305.
[35] T.J. Barnum, K.L.K. Lee, B.A. McGuire, Chirped-Pulse fourier transform millimeter-wave spectroscopy of furan, isotopologues, and vibrational excited states, ACS Earth Space Chem. 5 (11) (2021) 2986–2994.
[36] Z.-C. Wang, V.M. Bierbaum, Experimental and computational studies of the reactions of N and O atoms with small heterocyclic anions, J. Phys. Chem. A 121 (19) (2017) 3655–3661.
[37] A. Mellouki, J. Liévin, M. Herman, The vibrational spectrum of pyrrole ($C_4H_5N$) and furan ($C_4H_4O$) in the gas phase, Chem. Phys. 271 (3) (2001) 239–266.

[38] D.W. Tokaryk, S.D. Culligan, B.E. Billinghurst, J.A. van Wijngaarden, Synchrotron-based far-infrared spectroscopy of furan: Rotational analysis of the $\nu_{14}$, $\nu_{11}$, $\nu_{18}$ and $\nu_{19}$ vibrational levels, J. Mol. Spectrosc. 270 (1) (2011) 56–60.

[39] B. Pankoke, K. M. T. Yamada, G. Winnewisser, High resolution IR-spectra of Furane and Thiophene. Z. Naturforsch. 49a (1994), 1193–1202.

[40] L.W. Pickett, The Infra-Red spectrum of furan, J. Chem. Phys. 10 (11) (1942) 660–663.

[41] V. Barone, Vibrational spectra of large molecules by density functional computations beyond the harmonic approximation: the case of pyrrole and furan, Chem. Phys. Lett. 383 (2004) 528–532.

[42] P.R. Bunker, P. Jensen, Molecular Symmetry and Spectroscopy, 2nd ed., NRC Research Press, Ottawa, 2012.

[43] C.J.H. Schutte, J.E. Bertie, P.R. Bunker, J.T. Hougen, I. Mills, J.K.G. Watson, B. P. Winnewisser, Notations and Conventions in Molecular Spectroscopy: Part 2. Symmetry Notation, Pure Appl. Chem. 69 (1997) 1641–1649.

[44] B. Bak, D. Christensen, W.B. Dixon, L. Hansen-Nygaard, J. Rastrup Andersen, M. Schottländer, The complete structure of furan, J. Mol. Spectrosc. 9 (1962) 124–129.

[45] G.R. Tomasevich, K.D. Tucker, P. Thaddeus, Hyperfine structure of furan, J. Chem. Phys. 59 (1973) 131–135.

[46] F. Mata, M.C. Martin, G.O. Sørensen, Microwave spectra of deuterated furans. Revised molecular structure of furan, J. Mol. Struct. 48 (2) (1978) 157–163.

[47] G. Wlodarczak, L. Martinache, J. Demaison, B.P. Van Eijck, The Millimeter-Wave Spectra of Furan, Pyrrole, and Pyridine: Experimental and theoretical determination of the quartic centrifugal distortion constants, J. Mol. Spectrosc. 127 (1) (1988) 200–208.

[48] A. Mellouki, M. Herman, J. Demaison, B. Lemoine, L. Margulès, Rotational analysis of the $\nu_7$ band in furan ($C_4H_4O$), J. Mol. Spectrosc. 198 (1999) 348–357.

[49] A. Mellouki, J. Vander Auwera, J. Demaison, M. Herman, Rotational analysis of the $\nu_6$ band in furan ($C_4H_4O$), J. Mol. Spectrosc. 209 (2001) 136–138.

[50] G.G. Brown, B.C. Dian, K.O. Douglass, S.M. Geyer, S.T. Shipman, B.H. Pate, A broadband fourier transform microwave spectrometer based on chirped pulse excitation, Rev. Sci. Instrum. 79 (053103) (2008) 1–13.

[51] G.B. Park, R.W. Field, Perspective: The first ten years of broadband chirped pulse fourier transform microwave spectroscopy, J. Chem. Phys. 144 (200901) (2016) 1–10.

[52] P. Chen, S.D. Colson, W.A. Chupka, J.A. Berson, Flash Pyrolytic Production of Rotationally Cold Free Radicals in a Supersonic Jet. Resonant Multiphoton Spectrum of the $3p^2A_2'' \leftarrow X^2A_2''$ Origin Band of $CH_3$, J. Phys. Chem. 90 (1986) 2319–2321.

[53] B. J. Esselman, D. W. Tokaryk, R. C.Woods, R. J. McMahon, Unpublished Work.

[54] R.A. Loomis, A.M. Burkhardt, C.N. Shingledecker, S.B. Charnley, M.A. Cordiner, E. Herbst, S. Kalenskii, K.L.K. Lee, E.R. Willis, C. Xue, A.J. Remijan, M.C. Mccarthy, B.A. Mcguire, An investigation of spectral line stacking techniques and application to the detection of $HC_{11}N$, Nature Astronomy 5 (2021) 188–196.

[55] B.A. McGuire, R.A. Loomis, A.M. Burkhardt, K.L.K. Lee, C.N. Shingledecker, S. B. Charnley, I.R. Cooke, M.A. Cordiner, E. Herbst, S. Kalenskii, M.A. Siebert, E. R. Willis, C. Xue, A.J. Remijan, M.C. McCarthy, Detection of two interstellar polycyclic aromatic hydrocarbons via spectral matched filtering, Science 371 (2021) 1265–1269.

[56] M.D. Hanwell, D.E. Curtis, D.C. Lonie, T. Vandermeersch, E. Zurek, G.R. Hutchison, Avogadro: an advanced semantic chemical editor, visualization, and analysis platform, J. Cheminform. 4 (2012) 17.

[57] K. Prozument, G.B. Park, R.G. Shaver, A.K. Vasiliou, J.M. Oldham, D.E. David, J. S. Muenter, J.F. Stanton, A.G. Suits, G.B. Ellison, R.W. Field, Chirped-Pulse millimeter-wave spectroscopy for dynamics and kinetics studies of pyrolysis reactions, Phys. Chem. Chem. Phys. 16 (2014) 15739–15751.

[58] G.B. Guthrie, D.W. Scott, W.N. Hubbard, C. Katz, J.P. McCullough, M.E. Gross, K. D. Williamson, G. Waddington, Thermodynamic Properties of Furan, J. Am. Chem. Soc. 74 (18) (1952) 4662–4669.

[59] C.M. Western, PGOPHER: A Program for Simulating Rotational, Vibrational and Electronic Spectra, J. Quant. Spectrosc. Radiat. Transf. 186 (2017) 221–242.

[60] D.A. Matthews, L. Cheng, M.E. Harding, F. Lipparini, S. Stopkowicz, T.-C. Jagau, P. G. Szalay, J. Gauss, J.F. Stanton, Coupled-Cluster Techniques for Computational Chemistry: The CFOUR Program Package, J. Chem. Phys. 152 (214108) (2020) 1–35.

[61] J. Almlöf, P.R. Taylor, General contraction of Gaussian Basis Sets. I. Atomic Natural Orbitals for First-and Second-Row Atoms, J. Chem. Phys. 86 (7) (1987) 4070–4077.

[62] MATLAB. Matlab 2020. The MathWorks Inc. 2021.

[63] G.B. Park, A.H. Steeves, K. Kuyanov-Prozument, J.L. Neill, R.W. Field, Design and Evaluation of a Pulsed-Jet Chirped-Pulse Millimeter-Wave Spectrometer for the 70–102 GHz Region, J. Chem. Phys. 135 (024202) (2011) 1–10.

[64] R.A. Motiyenko, L. Margulès, E.A. Alekseev, J.-C. Guillemin, J. Demaison, Centrifugal distortion analysis of the rotational spectrum of aziridine: Comparison of different Hamiltonians, J. Mol. Spectrosc. 264 (2010) 94–99.

[65] L. Margulès, R.A. Motiyenko, E.A. Alekseev, J. Demaison, Choice of the reduction and of the representation in centrifugal distortion analysis: A case study of dimethylsulfoxide, J. Mol. Spectrosc. 260 (1) (2010) 23–29.

[66] W. Gordy, R.L. Cook, (Robert L, Wiley, Microwave Molecular Spectra, 1984.

[67] M.E. Sanz, M.C. McCarthy, P. Thaddeus, Vibrational excitation and relaxation of five polyatomic molecules in an electrical discharge, J. Chem. Phys. 122 (2005) 1–10.

[68] J.H. Baraban, D.E. David, G.B. Ellison, J.W. Daily, An optically accessible pyrolysis microreactor, Rev. Sci. Instrum. 87 (014101) (2016) 1–5.

[69] T. Erickson, Laser Spectroscopy of Acetylene, Massachusetts Institute of Technology (2020).

[70] J.E. Dickens, W.M. Irvine, M. Ohishi, M. Ikeda, S. Ishikawa, A. Nummelin, A. Hjalmarson, Detection of interstellar ethylene oxide (c-$C_2H_4O$), Astrophys. J. 489 (1997) 753–757.

[71] A. Nummelin, J.E. Dickens, P. Bergman, A. Hjalmarson, W.M. Irvine, M. Ikeda, M. Ohishi, Abundances of ethylene oxide and acetaldehyde in hot molecular cloud cores, A & A. 337 (1998) 275–286.

[72] B.A. McGuire, P. Brandon Carroll, R.A. Loomis, I.A. Finneran, P.R. Jewell, A. J. Remijan, G.A. Blake, Discovery of the Interstellar Chiral Molecule Propylene Oxide (CH3CHCH2O), Science 352 (6292) (2016) 1449–1452, https://doi.org/10.1126/science.aae0328.

[73] M.C. Mccarthy, B.A. Mcguire, Aromatics and cyclic molecules in molecular clouds: A new dimension of interstellar organic chemistry, J. Phys. Chem. A. 125 (2021) 3231–3243.

[74] B.A. McGuire, A.M. Burkhardt, S. Kalenskii, C.N. Shingledecker, A.J. Remijan, E. Herbst, M.C. McCarthy, Detection of the aromatic molecule benzonitrile (c-C6H5CN) in the interstellar medium, Science 359 (2018) 202–205.

[75] A.M. Burkhardt, K.L.K. Lee, P.B. Changala, C.N. Shingledecker, I.R. Cooke, R. A. Loomis, H. Wei, S.B. Charnley, E. Herbst, M.C. McCarthy, B.A. McGuire, Discovery of the Pure Polycyclic Aromatic Hydrocarbon Indene (c-C9H8) with GOTHAM Observations of TMC-1, The Astrophysical Journal Letters 913 (2) (2021) L18.

[76] T.J. Barnum, M.A. Siebert, K.L.K. Lee, R.A. Loomis, P.B. Changala, S.B. Charnley, M.L. Sita, C. Xue, A.J. Remijan, A.M. Burkhardt, B.A. McGuire, I.R. Cooke, A search for heterocycles in GOTHAM observations of TMC-1, J. Phys. Chem. A. 126 (2022) 2716–2728.

[77] A. Belloche, H.S.P. Müller, K.M. Menten, P. Schilke, C. Comito, Complex Organic Molecules in the Interstellar Medium: IRAM 30 m Line Survey of Sagittarius B2(N) and (M), A&A. 559 (2013) A47.

[78] A. Ginsburg, B. McGuire, R. Plambeck, J. Bally, C. Goddi, M. Wright, Orion SrcI's Disk Is Salty, Astrophys. J. 872 (2019) 54.